International Journal of Scientific Engineering and Applied Science (IJSEAS) - Volume-1, Issue-9, December 2015
ISSN: 2395-3470
www.ijseas.com

The Mechanism of the Occurrence of Possible High Temperature Granular Superconductivity in Carbon Materials

Takashi Kato
Institute for Innovative Science and Technology, Graduate School of Engineering, Nagasaki Institute of Applied Science, 3-1, Shuku-machi, Nagasaki 851-0121, Japan

Abstract

The reasonable mechanism of the occurrence of high-temperature superconductivity in the graphite powder treated by water or exposed to the hydrogen plasma, recently discovered, is discussed on the basis of recent experimental and our previous theoretical researches. Absorption of many additional materials with carbon framework by water treatment and expose to the hydrogen plasma plays an important role in the complete occupation of electrons in the valence bands, and furthermore, play an important role in the enlargement of the valence–conduction band gaps as a consequence of the increase of the sp^3-hybrid orbitals. Cooper pairs can be stabilized by large valence–conduction band gaps as a consequence of the quantization of the orbitals by nature at high-temperatures in these carbon materials. The guiding principles towards larger relative superconducting mass in these materials and towards high temperature superconductivity, are also suggested.

Keywords: Granular High Temperature Superconductivity; Alkane sp^3-Hybrid Orbitals; Alkene sp^2-Hybrid Orbitals; Graphite and Diamond.

1. Introduction

We have investigated the electron–phonon interactions in various charged molecular crystals for more than ten years. In particular, in 2002, we predicted the occurrence of superconductivity as a consequence of vibronic interactions in the negatively charged picene, phenanthrene, and coronene [1]. Recently, it was reported that these trianionic molecular crystals exhibit superconductivity [2]. According to these researches, however, it would be very difficult for the room temperature superconductivity as a consequence of electron–phonon interactions to be realized.

On the other hand, in the previous work, we discussed the relationship between the conventional superconducting state and the ring current [3–13] in these molecular systems (graphenes such as benzene (**6an**), naphthalene (**10ac**), anthracene (**14ac**), and tetracene (**18ac**), alkanes such as ethane (**2alka**), propane (**3alka**), butane (**4alka**), and pentane (**5alka**), and diamond-like alkanes such as C_5H_{12} (**5dia**) and $C_{14}H_{24}$ (**14dia**) [3–13]. Furthermore, we have predicted that the Cooper pairs can be formed by the large valence–conduction band gaps ($\Delta E_{\mathrm{HOMO-LUMO},N}$) as a consequence of the quantization of the orbitals by nature, and by the attractive Coulomb interactions between two electrons with opposite momentum and spins occupying the same orbitals via the positively charged nuclei [3–13]. Recently, Cooper pairs were excellently discovered at room temperatures in aromatic hydrocarbons such as **6an**, **10ac**, **14ac**, and coronene [14], as we predicted [3–13]. By analogy with the supercurrents in microscopic sized graphene molecule with large $\Delta E_{\mathrm{HOMO-LUMO},N}$ values, we predicted that the macroscopic sized materials with very large valence–conduction band gaps such as alkanes and diamonds, the valence bands of which are completely occupied by electrons, can exhibit superconductivity at the temperatures in the order of 10^4~10^5 K, theoretically [3–13].

In 2012, Esquinazi et al. reported that the virgin graphite powder treated by water or exposed to the hydrogen plasma can exhibit superconductivity at much higher temperatures than room temperatures [15]. Although the superconducting yield with their treatment is small (≈ 100 ppm), without exception, all prepared samples with the same powder showed superconducting behavior [15]. Furthermore, it was reported by Kawashima that ring current in a ring-shaped container into which n-octane-soaked thin graphite flakes were compressed did not decay for 50 days at room temperature [16].

In this article, on the basis of our previous theoretical works described above [3–13], which can be well confirmed by the recent experimental work [14], we show the reasonable mechanism of the occurrence of the high temperature superconductivity in the virgin graphite powder treated by water or exposed to the hydrogen plasma, discovered by Esquinazi et al [15]. We also suggest the guiding principle towards larger relative superconducting mass in these materials, and towards high temperature superconductivity.

2. Electronic Properties as a Function of the Applied Magnetic Field

Let us next consider how electronic properties are related to the applied magnetic field [15]. Coleman and

Heeger et al. [17] observed an extraordinary increase in conductivity just above the Peierls soft mode instability in an organic solid of tetrathiafulvalenium–tetracyanoquinodimethanide (TTF–TCNQ) in which the conduction is primarily along chains of molecules in essentially one dimension. In the previous works, by considering that the current–voltage characteristics observed between the critical temperatures of the Peierls distortions in the one-dimensional materials are very similar to those observed in the superconductor–insulator–superconductor tunneling junction materials at finite temperatures, and that there are generally intramolecular supercurrents in small molecules with closed-shell electronic structures at room temperature, we suggested that an extraordinary increase in conductivity observed by Coleman and Heeger et al. [17] as described above can be understood from the tunneling effects of the supercurrents between two neighboring TTF–TCNQ unit cells [18–20].

We define three important thermodynamic critical fields [18–20]. The energy levels for the valence and conduction bands in intragrains and intergrains are shown in Fig. 1. The $h_{c,inter}(T)$ value denotes the critical magnetic field, above which the tunneling intergranular supercurrents between two neighboring grains can start to be induced at T K. The $H_{c,inter}(T)$ value denotes the magnetic critical field, above which the intergranular supercurrents are destroyed at T K. The $H_{c,intra}(T)$ value denotes the critical field, above which the intragranular diamagnetic supercurrents can be destroyed at T K.

2.1 Intragranular Diamagnetic Supercurrents

At $H_{applied} < h_{c,inter}(0) << 157$ Oe [15], the intragranular diamagnetic supercurrents exist, according to the applied magnetic field $H_{applied}$, as shown in Figs. 1 (b) and 2 (b). On the other hand, the applied magnetic field $H_{applied}\left(< h_{c,inter}(0)\right)$ is too small for the tunneling intergranular supercurrents between two neighboring grains to be induced. This finite $h_{c,inter}(0)$ value needed originates from the fact that we consider granular superconductivity.

2.2 Intergranular Tunneling Supercurrents

In the intergranular supercurrents, two Josephson critical fields can be defined, namely, $H_{c,inter,lower}(T)$, i.e., the lower Josephson critical field as the characteristics field above which fluxons penetrate into the sample, and $H_{c,inter,upper}(T)$, the Josephson decoupling field above which the superconducting grains' response is the same as that of isolated superconducting grains at T K [15]. At a maximum applied field strength,

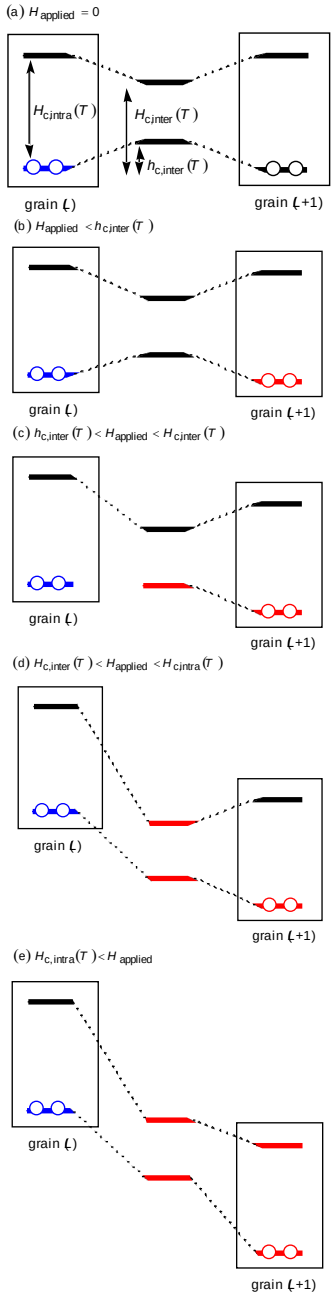

Fig. 1. Electronic structures as a function of the applied magnetic field. (a) $H_{applied} = 0$. (b) $H_{applied} < h_{c,inter}(T)$. (c) $h_{c,inter}(T) < H_{applied} < H_{c,inter}(T)$. (d) $H_{c,inter}(T) < H_{applied} < H_{c,intra}(T)$. (e) $H_{c,intra}(T) < H_{applied}$.

$h_{c,inter}(T) < H_{max} < H_{c,inter,lower}(T)$, no hysteresis or remanence is observed and the magnetization is given by

International Journal of Scientific Engineering and Applied Science (IJSEAS) - Volume-1, Issue-9, December 2015
ISSN: 2395-3470
www.ijseas.com

the macroscopic shielding currents (running through the weakly coupled grains) and the microscopic current loops

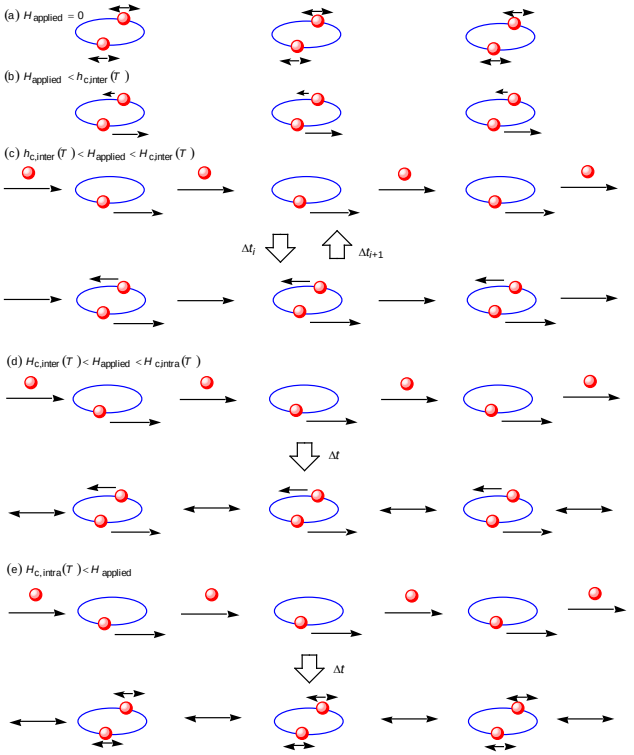

Fig. 2. Electrical currents as a function of the applied magnetic field. (a) $H_{\text{applied}} = 0$. (b) $H_{\text{applied}} < h_{\text{c,inter}}(T)$. (c) $h_{\text{c,inter}}(T) < H_{\text{applied}} < H_{\text{c,inter}}(T)$. (d) $H_{\text{c,inter}}(T) < H_{\text{applied}} < H_{\text{c,intra}}(T)$. (e) $H_{\text{c,intra}}(T) < H_{\text{applied}}$. In these figures, the large open circles indicate the grains, and small shaded circles indicate the electrons.

(circulating around the grains) within their corresponding penetration depths (Fig. 2 (c)). At $H_{\text{c,inter,lower}}(T) < H_{\max} < H_{\text{c,inter,upper}}(T)$, intergranular and London currents around the grains can trap fluxons as well as intragranular Abrikosov vortices. At $H_{\max} > H_{\text{c,inter,upper}}(T)$, there is a transition to a nonhysteretic mode and the magnetic moment in this field range is due to the flux expulsion from the isolated superconducting grains [15].

At $h_{\text{c,inter}}(0) < H_{\text{applied}} < H_{\text{c,inter,upper}}(0) \approx 663$ Oe , the tunneling intergranular supercurrents between two neighboring grains as well as the intragranular diamagnetic supercurrents can be induced, according to the applied magnetic field H_{applied}, as shown in Figs. 1 (c) and 2 (c).

Let us next look into the tunnel junction between two neighboring superconducting grains. In the superconducting state, an energy gap appears in the energy spectrum of the unpaired electrons, which strongly changes the density of states near the Fermi energy. No tunneling current can flow up to the applied magnetic field, $H_{\text{applied}}\left(< h_{\text{c,inter}}(0)\right)$, as shown in Fig. 2 (b). If the energy of intergranular electronic states between grains (L) and (L+1) is lowered compared to that of grain (L) by means of the magnetic field, at $H_{\text{applied}} = h_{\text{c,inter}}(0)$, a pair can be broken up (Figs. 1 (c) and 2 (c)). As a result, a single electron appears in the lowest state of grain (L), whereas the other electron tunnels into the lowest state of grain (L+1) via the intergranular electronic states between grains (L) and (L+1), as shown in Figs. 1 (c) and 2 (c). Only for a very short time, there are two electrons in the intergranular electronic states between grains (L) and (L+1), and these two electrons forming a pair are in the ground state (Fig. 2 (c)) as in the beginning. Similar discussions can be made between all two neighboring grains. The excitation of the one electron can be supplied by the transfer of the other electron in the magnetic field (Figs. 1 (c) and 2 (c)). During this process (Fig. 2 (c)), one of two electrons in all grains tunnels from the negative parts to the positive parts without energy loss. Therefore, we can observe the supercurrents in the whole localized grain with the valence bands completely occupied by electrons (Figs. 1 (c) and 2 (c)).

2.3 Destruction of the Intergranular Supercurrents

At 663 Oe $\approx H_{\text{c,inter,upper}}(0) < H_{\text{applied}} < H_{\text{c,intra}}(0)$, there is a transition to a nonhysteretic mode and the magnetic moment in this range is due to the flux expulsion from the isolated superconducting grains [15]. In this case, the intragranular diamagnetic supercurrents exist, according to the applied magnetic field H_{applied}, and electrons occupying the valence bands in grain (L) tunnel to the valence bands in the grain (L+1) at the beginning, as shown in Fig. 2 (d). However, in the process of tunneling, tunneling electrons are promoted from the valence to the conduction bands, and go through the conduction bands in granular materials with the size of the ten micrometers (Figs. 1 (d) and 2 (d)). Therefore, the intergranular tunneling electrical currents are immediately dissipated, and the macroscopic sized superconductivity in solids is destroyed (Fig. 2 (d)). Therefore, only intragranular superconductivity can remain (Fig. 2 (d)). This is the reason why the superconducting grains' response is the same as that of isolated superconducting grains at

663 Oe $\approx H_{\mathrm{c,inter,upper}}(0) < H_{\mathrm{applied}} < H_{\mathrm{c,intra}}(0)$, above the Josephson decoupling field.

The critical temperature $T_{\mathrm{c,inter,lower}}$ values, defined at $H_{\mathrm{c,inter,lower}}(T_{\mathrm{c,inter,lower}}) \to 0$ Oe, above which intergranular and London currents around the grains can trap fluxons as well as intragranular Abrikosov vortices, are estimated to be about $3 \sim 4 \times 10^3$ K [15]. The critical temperature $T_{\mathrm{c,inter,upper}}$ values, defined at $H_{\mathrm{c,inter,upper}}(T_{\mathrm{c,inter,upper}}) \to 0$ Oe, above which the tunneling intergranular currents between two neighboring grains are destroyed, are estimated to be very large, and about 10^4 K [15].

2.4 Destruction of the Intragranular Diamagnetic Supercurrents

At $H_{\mathrm{applied}} > H_{\mathrm{c,intra}}(0)$, we cannot neglect the second-order perturbation effects originating from the fact that electrons occupying the valence bands are promoted to the conduction bands in each grain. Therefore, the intragranular electrical currents are immediately dissipated, and thus intragranular as well as the intergranular supercurrents are destroyed (Fig. 2 (e)). Therefore, at $H_{\mathrm{applied}} > H_{\mathrm{c,intra}}(0)$, the intragranular diamagnetic supercurrents as well as the tunneling intergranular supercurrents between two neighboring grains are destroyed, as shown in Figs. 1 (e) and 2 (e).

3. Superconducting Critical Temperatures

The critical temperature $T_{\mathrm{c,intra,HOMO-LUMO},N}$ at which the ground states are transformed into the one-electron promoted excited states, which is related to the $\Delta E_{\mathrm{HOMO-LUMO},N}$ values of small hydrocarbons with N carbon atoms, can be expressed as

$$T_{\mathrm{c,intra,HOMO-LUMO},N} \propto \Delta E_{\mathrm{HOMO-LUMO},N} = \varepsilon_{\mathrm{LUMO},N} - \varepsilon_{\mathrm{HOMO},N}, \quad (1)$$

where the $\varepsilon_{\mathrm{LUMO},N}$ and $\varepsilon_{\mathrm{HOMO},N}$ values denote the orbital energy levels for the LUMO and HOMO in hydrocarbons with N carbon atoms, respectively.

The critical temperature $T_{\mathrm{c,intra,BCS},N}$ at which the conventional superconducting states are transformed to the normal metallic states of large hydrocarbons with N carbon atoms, can be expressed as

$$T_{\mathrm{c,intra,BCS},N} \propto e^{-1/\lambda_N}, \quad (2)$$

where the λ_N value denotes the dimensionless electron–phonon coupling constant in hydrocarbon with N carbon atoms [3–13].

The critical temperature $T_{\mathrm{c,intra},N}$ values for hydrocarbon with N carbon atoms can be defined as

$$T_{\mathrm{c,intra},N} = T_{\mathrm{c,intra,HOMO-LUMO},N} \quad \text{for large } \Delta E_{\mathrm{HOMO-LUMO},N}$$
$$= T_{\mathrm{c,intra,BCS},N} \quad \text{for small } \Delta E_{\mathrm{HOMO-LUMO},N}. \quad (3)$$

The $T_{\mathrm{c,intra,HOMO-LUMO},N}$ values (10^4~10^5 K) for the materials with large $\Delta E_{\mathrm{HOMO-LUMO},N}$ values are estimated to be much larger than the $T_{\mathrm{c,intra,BCS},N}$ values (10^0~10^2 K) for the materials with small $\Delta E_{\mathrm{HOMO-LUMO},N}$ values [3–13]. This can be understood as follows. In the conventional superconductivity, the $\Delta E_{\mathrm{HOMO-LUMO},N}$ value is usually very small, and thus even in the closed-shell electronic states, electron pairs formed by two electrons occupying the same molecular orbitals are destroyed by vibration of nuclei. Therefore, in the conventional superconductivity, the electron pairing would not be formed by nature and the energy lowering $\Delta(0)_{\mathrm{BCS},N}$ as a consequence of electron–phonon interactions is needed in order that the Bose–Einstein condensation states and superconducting states which are more stable than the normal metallic Fermi states are realized. Furthermore, in the conventional superconductivity, such energy lowering factor originating from the attractive electron–electron interactions λ_N appears in the exponential factor in the equation for $T_{\mathrm{c,intra,BCS},N}\left(\propto \Delta(0)_{\mathrm{BCS},N} \propto e^{-1/\lambda_N}\right)$. Such an exponential factor appears because electronic states are very close each other in the conventional superconductors with macroscopic sizes, and we must consider energy-space or ***k***-space integrals continuously in a thin shell around the Fermi-surface. Therefore, such energy lowering $\Delta(0)_{\mathrm{BCS},N}$ originating from electron–phonon interactions is very small. On the other hand, in the microscopic sized hydrocarbon molecules, the $\Delta E_{\mathrm{HOMO-LUMO},N}$ value is very large. Because of the discrete energy levels between the valence and conduction bands, electron pairs cannot be easily destroyed in the microscopic sized hydrocarbon molecules, and not $V_{\mathrm{Coulomb},N}$ but $\Delta E_{\mathrm{HOMO-LUMO},N}$, which is much larger than the $\Delta(0)_{\mathrm{BCS},N}$ values, becomes the $T_{\mathrm{c,intra,HOMO-LUMO},N}$. Furthermore, even if the attractive electron–electron interactions are very small, electron pair can be formed. Therefore, the strengths of

International Journal of Scientific Engineering and Applied Science (IJSEAS) - Volume-1, Issue-9, December 2015
ISSN: 2395-3470
www.ijseas.com

the attractive electron–electron interactions originating from the Coulomb interactions are not directly related to the $T_{c,intra,HOMO-LUMO,N}$ values in the microscopic sized hydrocarbons. We can consider that electron pairs formed by two electrons occupying the same orbital are provided by nature in the closed electronic structures with large energy gaps between the occupied and unoccupied orbitals such as polyacenes, annulenes, He atoms, and pure diamonds [3–13]. In summary, energy lowering factor λ_N in the equation for $T_{c,intra,BCS,N}$ and very small $\Delta E_{HOMO-LUMO,N}$ values, originating from continuous energy levels of electronic states in the conventional superconductors with the macroscopic sizes, and the energy gap between the ground and excited states which is proportional to the very large $\Delta E_{HOMO-LUMO,N}$ and $T_{c,intra,HOMO-LUMO,N}$ values, originating from discrete energy levels of electronic states in the microscopic sized hydrocarbons, are the main reasons that the $T_{c,intra,HOMO-LUMO,N}$ values for the microscopic sized hydrocarbons are estimated to be much larger than the $T_{c,intra,BCS,N}$ values for the macroscopic sized conventional superconductors.

4. The Role of Waters and Hydrogen Plasma in the Occurrence of Superconductivity

It was reported that room temperature superconducting behavior is observed in the graphite powder treated by water or exposed to the hydrogen plasma [15]. This means that we can consider that hydrogen atoms and water molecules play an essential role in the occurrence of superconducting behavior in these carbon materials.

Let us discuss how hydrogen atoms and water molecules play an important role in the electronic structures in these carbon materials. We define the $p_{saturated}$ value denoting the ratio of the number of carbon atoms with saturated sp^3 hybrid orbitals to that of the total carbon atoms located in the area directly related to the superconductivity. In untreated virgin graphite powder ($p_{saturated} = 0$), there are some impurities. Therefore, there are some holes in valence bands in untreated virgin graphite powder, as shown in Fig. 3 (a). Furthermore, in untreated virgin graphite powder ($p_{saturated} = 0$), there are many π-conjugated carbons originating from sp^2 hybrid orbitals. Therefore, the $\Delta E_{HOMO-LUMO,N}$ values for materials with N carbon atoms are very small (≈ 0.0 eV). In such a case, the electronic states can be in the normal metallic states. This is the reason why the superconductivity has not been observed in the untreated virgin graphite powder ($p_{saturated} = 0$).

On the other hand, in the graphite powder treated by water or exposed to hydrogen plasma, first, hydrogen atoms and part of water molecules (for example, hydrogen atoms and hydroxyl group) can be completely terminated with carbon framework ($p_{saturated} = 0$). Therefore, the valence bands are completely occupied by electrons, as shown in Fig. 3 (a). If completely terminated π-conjugated graphite compounds ($p_{saturated} = 0$) are formed, the valence bands are completely occupied by

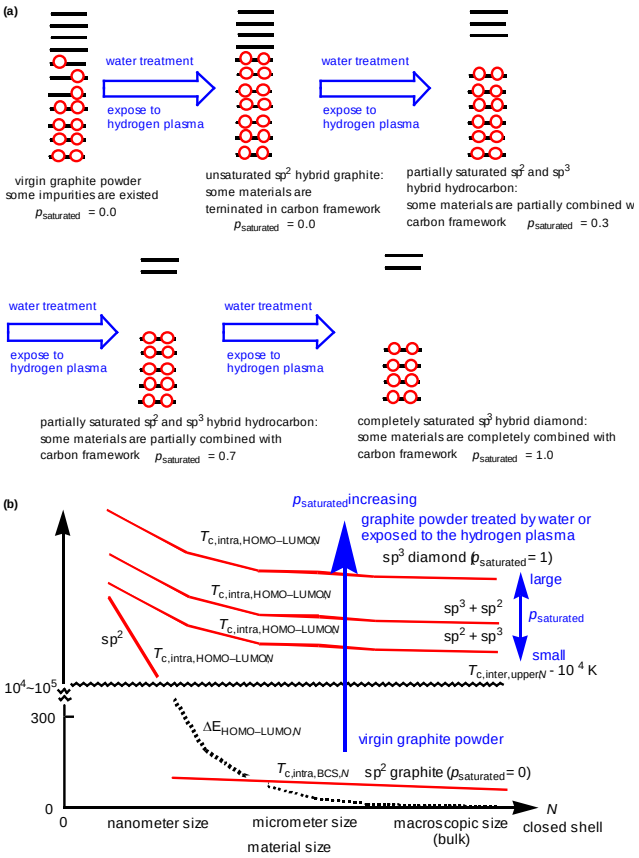

Fig. 3. (a) Changes of electronic structures by water treatment or expose to the hydrogen plasma in the virgin graphite powder. (b) Superconducting critical temperatures as a function of material size in sp^2- and sp^3-type hybrid hydrocarbons. In this figure, a wave indicates the $T_{c,inter,upper}$ values of about 10^4 K, solid lines indicate the superconducting critical temperatures, and a dotted line indicates the HOMO–LUMO gap for sp^2-type hybrid hydrocarbons.

electrons, on the other hand, the $\Delta E_{HOMO-LUMO,N}$ values are still very small (≈ 0.0 eV) with a grain size of several tens of micrometers.

If many hydrogen atoms and part of water molecules are absorbed in the virgin graphite powder, there is a

possibility that the alkane parts originating from the sp^3 hybrid orbitals as well as the alkene parts originating from the sp^2 hybrid orbitals can be formed. The $p_{\text{saturated}}$ value increases with an increase in the number of these additional materials combined with carbon framework. The $\Delta E_{\text{HOMO–LUMO},N}$ value increases with an increase in the $p_{\text{saturated}}$ value, as shown in Fig. 3 (a). Therefore, the $\Delta E_{\text{HOMO–LUMO},N}$ value increases with an increase in the number of these additional materials combined with carbon framework, as shown in Fig. 3 (a). In the virgin graphite powder exposed to the hydrogen plasma, the only hydrogen atoms are surely combined with the carbon framework in the graphite powder. On the other hand, in the water-treated graphite powder, whether water molecules, hydrogen atoms, hydroxyl group, or oxygen atoms can be combined with carbon framework are not clarified. However, we can at least say that the $p_{\text{saturated}}$ value increases with an increase in the number of these additional materials (whatever they are) combined with carbon framework.

In summary, absorption of many additional materials with carbon framework by water treatment and expose to hydrogen plasma in the virgin graphite powder plays an important role in the complete occupation of electrons in the valence bands, and furthermore, plays an important role in the enlargement of the $\Delta E_{\text{HOMO–LUMO},N}$ values as a consequence of the increase of the sp^3-hybrid orbitals.

5. Superconducting Critical Temperatures in Carbon Materials

5.1 Superconducting Critical Temperatures as a Function of the Valence–Conduction Band Gaps

Let us next discuss the critical temperatures $T_{\text{c,intra},N}$ at which the intragranular diamagnetic supercurrents can disappear in π-conjugated sp^2-type graphene hydrocarbons and sp^3-type alkane hydrocarbons with N carbon atoms, on the basis of recent experimental [15] and our previous theoretical [3–13] researches.

According to our previous researches [3–13], in the materials with large $\Delta E_{\text{HOMO–LUMO},N}$ values, the closed-shell electronic structures with large $\Delta E_{\text{HOMO–LUMO},N}$ values are formed by the quantization of orbitals by nature, and the attractive interactions between two electrons with opposite momentum and spins occupying the same orbitals can be realized by the Coulomb interactions between all nuclei and electrons. That is, in the materials with large $\Delta E_{\text{HOMO–LUMO},N}$ values, the Cooper pairs are formed by the large $\Delta E_{\text{HOMO–LUMO},N}$ values as a consequence of the quantization of the orbitals by nature, and by the attractive Coulomb interactions between two electrons with opposite momentum and spins occupying the same orbitals via the positively charged nuclei. The energy levels of the HOMO ($\varepsilon_{\text{HOMO},N}$) in the neutral **6an**, **10ac**, and **14ac** are about –10 eV, and the attractive Coulomb interactions between two electrons occupying the HOMO ($V_{\text{Coulomb,HOMO},N}$) in the neutral **6an**, **10ac**, and **14ac** were calculated to be about –70 eV in our previous researches [3–13].

On the other hand, according to the recent experimental research, the Cooper pairs have been observed at room temperatures in the neutral **6an**, **10ac**, **14ac**, and coronene [14]. The energies of the double-photoionization in the neutral **6an**, **10ac**, and **14ac** observed from the photoemission experiments are about 20~25 eV [14], which are similar to about the $-2\varepsilon_{\text{HOMO},N}(\approx 20\ \text{eV})$ values [3–13], and the destruction energies of the Cooper pairs in the neutral **6an**, **10ac**, and **14ac** observed from the photoemission experiments are about 70 eV [14], which are similar to the $-V_{\text{Coulomb,HOMO},N}(\approx 70\ \text{eV})$ values [3–13].

The energies for photoionization (approximately half of the double photoionization ($-\varepsilon_{\text{HOMO},N}\left(\sim \Delta E_{\text{HOMO–LUMO},N}(\approx 10\ \text{eV})\right)$)) [14] are related to the $T_{\text{c,intra},N}\left(\sim \Delta E_{\text{HOMO–LUMO},N}\left(\approx 10\ \text{eV} \approx 10^4 \sim 10^5\ \text{K}\right)\right)$ values [3–13], and the destruction energies of the Cooper pairs (70 eV) [14] are closely related to the $-V_{\text{Coulomb,HOMO},N}(\approx 70\ \text{eV})$ values [3–13]. That is, our prediction in our theoretical researches [3–13] can be well confirmed by the recent experimental research [14], and our previous theory [3–13] can be reasonably applied to the explanation of the mechanism of the occurrence of the granular high temperature superconductivity in carbon materials under consideration in this study.

On the other hand, the second-order perturbation effect as a consequence of one electron promotion from the HOMO to the LUMO becomes more important with a decrease in the $\Delta E_{\text{HOMO–LUMO},N}$ value. In such a case, the conventional BCS theory should be applied, and the electron–phonon interactions play an essential role in the forming of energy gap and the decision of the $T_{\text{c,intra},N}$ value (10^0~10^2 K).

The possible $T_{\text{c,intra},N}$ values as a function of the material size are shown in Fig. 3 (b). The critical temperature $T_{\text{c,intra},N}$ at which the intragranular diamagnetic supercurrents in carbon powder under consideration can disappear can be estimated to be larger than $T_{\text{c,inter,upper}} \approx 10^4$ K. The critical temperature

$T_{c,intra,N}$ values for hydrocarbon with N carbon atoms can be defined by Eq. (3). The $T_{c,intra,HOMO-LUMO,N}$ values (10^4~10^5 K) for the materials with large $\Delta E_{HOMO-LUMO,N}$ values are estimated to be much larger than the $T_{c,intra,BCS,N}$ values (10^0~10^2 K) for the materials with small $\Delta E_{HOMO-LUMO,N}$ values [3–13].

5.2 sp^2-Type Alkene Hydrocarbons

Let us discuss the $T_{c,intra,N}$ values for sp^2-type alkene hydrocarbons. In small sized molecules, the large energy gaps between the HOMO and LUMO (10^4~10^5 K) are formed by nature, by which the electron pairs formed by attractive Coulomb interactions between two electrons occupying the same orbital with opposite momentum and spins via the positive charges of nuclei become stabilized (Fig. 3 (b)) [3–13]. On the other hand, the $\Delta E_{HOMO-LUMO,N}$ value decreases with an increase in molecular size. Actually, the $\Delta E_{HOMO-LUMO,N}$ values for **10ac**, **14ac**, **18ac**, pentacene (**22ac**), and hexacene (**26ac**) are estimated to be 7.97, 6.93, 5.89, 5.35, and 2.98 eV, respectively, those for nanosized graphene are estimated to be about 0.35 eV, and furthermore, those for macroscopic sized graphite become nearly 0.0 eV [3–13]. Therefore, the second-order perturbation effect as a consequence of one electron promotion from the HOMO to the LUMO becomes more important with an increase in the molecular size. In such a case, the conventional BCS theory should be applied, and the electron–phonon interactions play an essential role in the forming of energy gap (10^0~10^2 K), as shown in Fig. 3 (b).

On the other hand, the $\Delta E_{HOMO-LUMO,N}$ value should be larger than the experimental $T_{c,inter,upper}$ values of 10^4 K (a few eV) (Fig. 3 (b)) [3–13]. Therefore, according to our calculations and experimental results [3–13,15], the material sizes for the π-conjugated sp^2-type graphene hydrocarbons must be smaller than the nano-size in order that the $T_{c,intra,N}$ values for these materials are larger than the experimental values of $T_{c,inter,upper} \approx 10^4$ K [15], shown as a wave in Fig. 3 (b). On the other hand, in such a case, very large number of Josephson links ($\approx N_{CH}$) is needed in each grain, as shown in Fig. 4.

5.3 sp^3-Type Alkane Hydrocarbons

Let us next discuss the $T_{c,intra,N}$ values for sp^3-type alkane hydrocarbons. The $\Delta E_{HOMO-LUMO,N}$ values are estimated to be 12.11, 11.47, 10.97, 11.00, 10.62, and 9.28 eV (140530, 133103, 127301, 127649, 123239, and 107589 K) for **2alka**, **3alka**, **4alka**, **5alka**, **5dia**, and **14dia**, respectively. Furthermore, the $\Delta E_{HOMO-LUMO,N}$ value for diamond with even macroscopic size is very large, 5.47 eV (63476 K) [3–13]. Therefore, the $\Delta E_{HOMO-LUMO,N}$ value does not significantly decrease with an increase in material size in sp^3-type alkane hydrocarbons and diamonds, as shown in Fig. 3 (b). The $\Delta E_{HOMO-LUMO,N}$ values are very large (5.47 eV) and the energy levels of the occupied orbitals are always

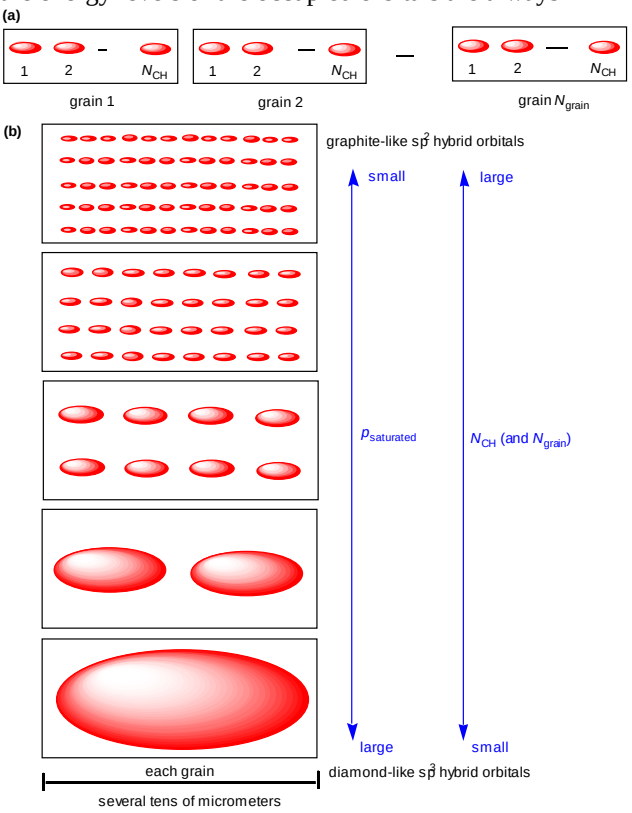

Fig. 4. The possible number of molecules in each grain. (a) The definitions of N_{grain} grains, and those of N_{CH} carbon molecules existed in each grain. (b) The possible minimum numbers of molecules in each grain as a function of the $p_{saturated}$ value.

negative ($\varepsilon_{orbital,N,j} < 0$) in diamonds, and thus the Coulomb energy between two electrons occupying the same orbitals via the positive charges of the nuclei can become large negative [3–13]. Therefore, by analogy with the supercurrents [3–13] and discovery of forming of the Cooper pairs [3–13] in the microscopic sized molecules such as **6an**, **10ac**, **14ac**, and coronene with large $\Delta E_{HOMO-LUMO,N}$ values, if we consider diamond as a macroscopic sized molecule with large $\Delta E_{HOMO-LUMO,N}$ values, we can expect that the superconductivity can be induced in the macroscopic

sized diamonds, the valence bands of which are completely occupied by electrons, at 300 K, as described in the previous researches [3–13]. Therefore, the $T_{c,intra,N}$ values for any size of sp^3-type alkane hydrocarbons can be larger than $T_{c,inter,upper} \approx 10^4$ K [15].

6. Guiding Principle towards Higher Relative Superconducting Masses

Let us consider the case where there are N_{grain} grains, and there are N_{CH} molecules in each grain, as shown in Fig. 4 (a). We can consider that there are about N_{CH} Josephson links between two neighboring molecules in each grain, about N_{grain} Josephson links between two neighboring grains, and totally about $N_{CH}N_{grain}$ Josephson links in granular materials with the size of the ten micrometers under consideration. As described above, if each grain is formed by only π-conjugated graphenes, we must consider that there are many small (smaller than nano-sized molecules) sized π-conjugated molecules with large $\Delta E_{HOMO-LUMO,N}$ values (larger than a few eV, at the smallest) in each grain, as shown in Fig. 4 (a). In such a case, very large numbers of nanosized π-conjugated hydrocarbons and Josephson links are needed in each grain with the size of several tens of micrometers, and thus the N_{CH} values should be very large, as shown in Fig. 4 (b). Such large number of Josephson junctions ($\approx N_{CH}$) would cause the small relative superconducting masses.

On the other hand, it is also possible that there is only one sp^3 diamond-type alkane hydrocarbon ($N_{CH} = 1$) with large $\Delta E_{HOMO-LUMO,N}$ value of 10^4~10^5 K in each grain with the sizes of the order of several tens of micrometers, as shown in Fig. 4. Furthermore, the $p_{saturated}$ value increases with an increase in the number of additional materials combined with carbon framework, as shown in Fig. 3 (a). The $\Delta E_{HOMO-LUMO,N}$ value for each molecule increases with an increase in the $p_{saturated}$ value (Fig. 3 (b)). The needed number of Josephson links N_{CH} in the hydrocarbons in each grain decreases with an increase in the $p_{saturated}$ value as a consequence of the increase in the number of additional materials combined with carbon framework, as shown in Figs. 3 (b) and 4 (b). If the $p_{saturated}$ value becomes large enough, only one hydrocarbon with sp^2- and sp^3-type hybrid characteristics with $\Delta E_{HOMO-LUMO,N}$ values in the order of 10^4~10^5 K is needed in each grain ($N_{CH} = 1$), as shown in Fig. 4 (b).

Even though we cannot clearly show which kind of structure or stoichiometry the superconducting grain part has, it is natural to conclude that the hydrocarbons with significant sp^3 characteristics rather than the sp^2 characteristics, the $\Delta E_{HOMO-LUMO,N}$ values of which are larger than a few eV, and the valence bands of which are completely occupied by electrons, are formed by water treatment or expose to the hydrogen plasma in the virgin graphite powder, as shown in Fig. 5.

Let us next consider how to reduce the number of intergranular Josephson links N_{grain} between two

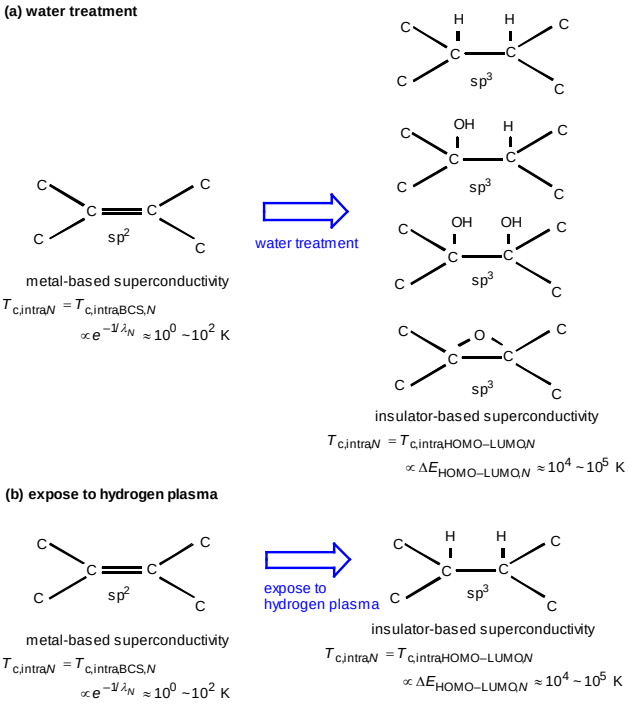

Fig. 5. Relationship between absorption of substituent groups in the virgin graphite powder and superconductivity. (a) Water treatment. (b) Expose to hydrogen plasma.

neighboring grains in solids. If the $p_{saturated}$ value becomes large enough, only one hydrocarbon with $\Delta E_{HOMO-LUMO,N}$ values in the order of 10^4~10^5 K is needed in the macroscopic sized solids. For example, the virgin diamond treated by water or exposed to the hydrogen plasma ($N_{CH} = 1$ and $N_{grain} = 1$) in a macroscopic sized grain, in which the valence bands are completely occupied by electrons, has a possibility to exhibit high-temperature superconductivity.

In general, regardless of the kinds of additional materials combined with carbon framework, the macroscopic sized materials with larger $\Delta E_{HOMO-LUMO,N}$ values than a few eV, in which the

valence bands are completely occupied by electrons (on the other hand, conduction bands can be also partially occupied by electrons), have a possibility to exhibit room temperature superconductivity ($N_{\mathrm{CH}} N_{\mathrm{grain}} = 1$).

7. Guiding Principle towards High Temperature Superconductivity

Let us next summarize the guiding principle towards the syntheses of high temperature superconductivity [3–13]. We can expect that any material with large $\Delta E_{\mathrm{HOMO-LUMO},N}$ value (more than a few eV) in which valence bands are completely occupied by electrons, which has been believed to be typical insulator in view of solid state physics and chemistry, has a possibility to exhibit high temperature superconductivity ($T_{\mathrm{C}} \approx 10^4$~$10^5$ K) in solids, as shown in Fig. 6. In these cases, it is also possible that the conduction bands are somewhat occupied by electrons even though electrons occupying not the conduction bands but the valence bands play an essential role in supercurrent. If some appropriate additional materials are combined enough with these materials so that the valence bands are completely occupied by electrons, these materials can exhibit high temperature superconductivity in solids. Furthermore, in such cases, finite magnetic field for intergranular tunneling effects is not needed ($h_{\mathrm{c,inter}}(0) = 0$). Discovery of appropriate combination of additional materials with the macroscopic sized main materials, by which the $\Delta E_{\mathrm{HOMO-LUMO},N}$ value becomes larger than a few eV, and by which the valence bands are completely occupied by electrons, is awaited.

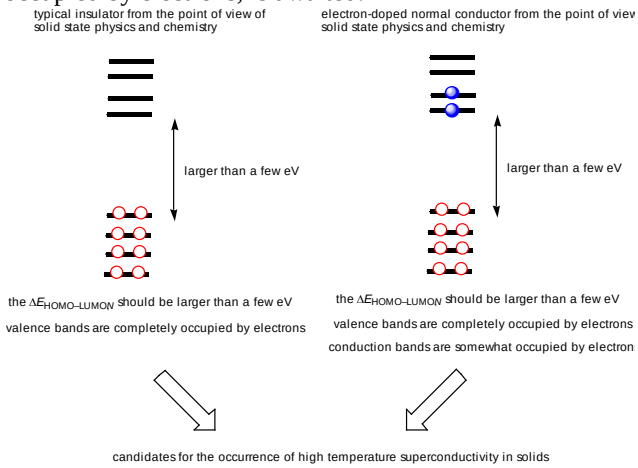

Fig. 6. The possible appropriate electronic structures for high temperature superconductivity. In this figure, the open and shaded circles indicate electrons occupying the valence and conduction bands, respectively.

According to recent work [21,22], graphene terminated with substituent, the $p_{\mathrm{saturated}}$ value of which is larger than about 0.35 have enough large $\Delta E_{\mathrm{HOMO-LUMO},N}$ value so that these materials can be considered to be insulator from the point of view of solid state physics. Therefore, according to our theory, substituted graphene with $p_{\mathrm{saturated}} (\geq 0.35)$ has a possibility to exhibit room temperature superconductivity.

8. Concluding Remarks

We investigated the reasonable mechanism of the occurrence of granular high temperature superconductivity in the graphite powder treated by water or exposed to the hydrogen plasma, discovered by Esquinazi et al. [15], on the basis of our previous theoretical works described above [3–13], which can be well confirmed by the recent experimental work [14]. We also suggested the guiding principle towards larger relative superconducting mass in these materials. Furthermore, we also suggested the general guiding principle towards high temperature superconductivity.

We first try to elucidate the essential role of water treatments and expose to the hydrogen plasma in decision of the electronic structures in untreated virgin graphite powder. We showed that absorption of many additional materials with carbon framework by water treatment and expose to hydrogen plasma in the virgin graphite powder plays an important role in the complete occupation of electrons in the valence bands, and furthermore, plays an important role in the enlargement of the $\Delta E_{\mathrm{HOMO-LUMO},N}$ values as a consequence of the increase of the sp^3-hybrid orbitals.

We next investigate the critical temperature for the intragranular diamagnetic supercurrents, on the basis of the recent experimental [14,15] and our previous theoretical [3–13] researches. According to these researches, in the materials with large $\Delta E_{\mathrm{HOMO-LUMO},N}$ values, the closed-shell electronic structures with large band gaps between the occupied and unoccupied orbitals are formed by the quantization of orbitals by nature, and the attractive interactions between two electrons with opposite momentum and spins occupying the same orbitals can be realized by the Coulomb interactions between all nuclei and electrons. That is, in the materials with large $\Delta E_{\mathrm{HOMO-LUMO},N}$ values, the Cooper pairs are formed by large $\Delta E_{\mathrm{HOMO-LUMO},N}$ values as a consequence of the quantization of the orbitals by nature, and by the attractive Coulomb interactions between two electrons with opposite momentum and spins occupying the same orbitals via the positively charged nuclei. These results can be well confirmed by the recent experimental results [14] that the Cooper pairs have been observed in the neutral **6an**, **10ac**, **14ac**, and coronene. We showed that if the $p_{\mathrm{saturated}}$ value becomes large enough, only

one hydrocarbon with sp^2- and sp^3-type hybrid characteristics with the $\Delta E_{\mathrm{HOMO-LUMO},N}$ values of a few eV is needed in each grain. Even though we cannot clearly show which kind of stoichiometry the superconductivity grain part has, it is natural to consider that the hydrocarbons with significant sp^3 characteristics rather than the sp^2 characteristics, the valence–conduction band gaps of which are larger than a few eV, and the valence bands of which are completely occupied by electrons, are formed by water treatment or expose to the hydrogen plasma in the virgin graphite powder.

We next suggest the guiding principle towards larger relative superconducting mass. For example, the virgin diamond treated by water or exposed to the hydrogen plasma in a macroscopic sized grain, in which the valence bands are completely occupied by electrons, have a possibility to exhibit high-temperature superconductivity. In general, regardless of the kinds of additional materials combined with carbon framework, the macroscopic sized materials with larger $\Delta E_{\mathrm{HOMO-LUMO},N}$ values than a few eV, in which the valence bands are completely occupied by electrons, have a possibility to exhibit high temperature superconductivity. Discovery of appropriate combination of additional materials with the main carbon materials, by which the $p_{\mathrm{saturated}}$ value becomes large enough, is awaited.

Finally, we suggest the guiding principle towards the syntheses of high temperature superconductivity. We suggest that any material with large $\Delta E_{\mathrm{HOMO-LUMO},N}$ value (more than a few eV), in which valence bands are completely occupied by electrons, which has been believed to be typical insulator in view of solid state physics and chemistry, has a possibility to exhibit high temperature superconductivity in solids.

Acknowledgments

This work is supported by The Iwatani Naoji Foundation's Research Grant.

References

[1] T. Kato, K. Yoshizawa, and K. Hirao, "Electron-phonon coupling in negatively charged acene- and phenanthrene-edge-type hydrocarbons" J. Chem. Phys. vol. 116, 2002, pp. 3420-3429.

[2] R. Mitsuhashi, Y. Suzuki, Y. Yamanari, H. Mitamura, T. Kambe, N. Ikeda, H. Okamoto, A. Fujiwara, M. Yamaji, N. Kawasaki, Y. Maniwa, and Y. Kubozono, "Superconductivity in alkali-metal-doped picene". Nature vol. 464, 2010, pp. 76-79.

[3] T. Kato, "Diamagnetic currents in the closed-shell electronic structures in sp^3-type hydrocarbons," Chemical Physics, vol. 345, 2008, pp. 1–13.

[4] T. Kato, "The essential role of vibronic interactions in electron pairing in the micro- and macroscopic sized materials," Chemical Physics, vol. 376, 2010, pp. 84–93.

[5] T. Kato, "The role of phonon- and photon-coupled interactions in electron pairing in solid state materials," Synthetic Metals, vol. 161, 2011, pp. 2113–2123.

[6] T. Kato, "New Interpretation of the role of electron-phonon interactions in electron pairing in superconductivity," Synthetic Metals, vol. 181, 2013, pp. 45–51.

[7] T. Kato, "The mechanism of occurrence of diamagnetic intramolecular ring currents in the neutral annulenes" Chemical Physics Research Journal, vol. 1, 2007, pp. 61–96, Nova Science Publishers, New York.

[8] T. Kato and T. Yamabe, "Intramolecular ring current in $(4n+2)\pi$ electronic states in the neutral acenes" Synthetic Metals vol. 157, 2007, pp.793–806.

[9] T. Kato and T. Yamabe, "Diamagnetic Currents in the Neutral He atoms" Journal of Physical Chemistry A vol. 111, 2007, pp.8731–8740.

[10] T. Kato, "Intramolecular Diamagnetic Currents in the Microscopic Sized Neutral Polyacetylenes" Journal of Physical Chemistry C vol. 113, 2009, pp.402–414.

[11] T. Kato, "Relationships between the intrinsic properties of electrical currents and temperatures," Proceedings of Eleventh TheIIER International Conference, February 2015, Singapore, pp. 63–68.

[12] T. Kato, "Relationships between the nondissipative diamagnetic currents in the microscopic sized atoms and molecules and the superconductivity in the macroscopic sized solids," Proceedings of Eleventh TheIIER International Conference, February 2015, Singapore, pp. 69–80.

[13] T. Kato, "Vibronic stabilization under the external applied fields," Proceedings of Eleventh TheIIER International Conference, February 2015, Singapore.

[14] R. Wehlitz, P. N. Juranic, K. Collins, B. Reilly, E. Makoutz, T. Hartman, N. Appathurai, S. B. Whitfield, Physical Review Letters "Photoemission of Cooper Pairs from Aromatic Hydrocarbons" vol. 109, 2012, 193001.

[15] T. Scheike, W. Böhlmann, P. Esquinazi, J. Barzola-Quiquia, A. Ballestar, A. Setzer, "Can Doping Graphite Trigger Room Temperature Superconductivity? Evidence for Granular High-Temperature Superconductivity in Water-Treated Graphite Powder" Advanced Materials, vol. 24, 2012, pp. 5826-5831.

[16] Y. Kawashima, "Possible room temperature superconductivity in conductors obtained by bringing alkanes into contact with a graphite surface" AIP Advances vol. 3, 2013, 052132.

[17] L. B. Coleman, M. J. Cohen, D. J. Sandman, F. G. Yamagishi, A. F. Garito, A. J. Heeger, "Superconducting Fluctuations and the Peierls Instability in an Organic

Solid" Solid State Communications vol. 12, 1973, pp. 1125-1132.
[18] T. Kato, "Tunneling Effects of the Nondissipative Diamagnetic Currents in the Negatively Charged One-Dimensional Tetracyanoquinodimethanide (TCNQ) Molecular Crystals" Journal of Physical Chemistry C vol. 113, 2009, pp. 19645-9657.
[19] T. Kato, "Non-Ohmic current-voltage characteristics in the positively charged tetrathiafulvalene (TTF) molecular crystals" Synthetic Metals vol. 161, 2011, 704-712.
[20] T. Kato, "New method of accurate estimation of the electron–phonon coupling constants in fractionally charged incommensurate electronic sates in molecular systems" Journal of Chemical Physics vol. 135, 2011, 024103.
[21] S. Obata, H. Tanaka, and K. Saiki "Electrical and Spectroscopic Investigations on the Reduction Mechanism of Graphene Oxide" vol. 55, 2013, pp. 126-133.
[22] H. Tanaka, S. Obata, and K. Saiki, "Reduction of Graphene Oxide in Solution by Radical Treatment" Chem. Lett. November, 2013, pp. 1-3.

Author Profile

Dr. Takashi Kato is a Professor at Nagasaki Institute of Applied Science, Japan. He completed his doctorate in physical chemistry with the theory of vibronic interactions and Jahn–Teller effects at Kyoto University (PhD (Engineering)), Japan, in 2000. During October 2001-February 2003, he has performed research concerning prediction of the occurrence of superconductivity of graphene-like aromatic hydrocarbons such as phenanthrene, picene, and coronene at Max-Planck-Institute for Solid State Research in Stuttgart, Germany, as a visiting scientist. In 2010, his prediction of the occurrence of superconductivity of picene and coronene were experimentally confirmed at Okayama University, Japan, and in 2011, that of phenanthrene was experimentally confirmed at University of Science and Technology of China. His theory and calculations concerning the guiding principle towards high-temperature superconductivity are highly regarded and recently reported several times in newspaper (The Nikkei), which is the most widely read in Japan, as follows ((1) July 8, 2014, The Nikkei; (2) October 19, 2013, The Nikkei; (3) November 7, 2011, The Nikkei; (4) January 14, 2011, The Nikkei; (5) November 22, 2010, The Nikkei; (6) November 18, 2010, The Nikkei).